Accepted Manuscript

An enhanced chemiluminescence resonance energy transfer aptasensor based on rolling circle amplification and WS_2 nanosheet for *Staphylococcus aureus* detection

Liling Hao, Huajie Gu, Nuo Duan, Shijia Wu, Xiaoyuan Ma, Yu Xia, Zui Tao, Zhouping Wang

PII: S0003-2670(17)30017-X

DOI: 10.1016/j.aca.2016.12.045

Reference: ACA 234989

To appear in: *Analytica Chimica Acta*

Received Date: 21 November 2016

Revised Date: 28 December 2016

Accepted Date: 30 December 2016

Please cite this article as: L. Hao, H. Gu, N. Duan, S. Wu, X. Ma, Y. Xia, Z. Tao, Z. Wang, An enhanced chemiluminescence resonance energy transfer aptasensor based on rolling circle amplification and WS_2 nanosheet for *Staphylococcus aureus* detection, *Analytica Chimica Acta* (2017), doi: 10.1016/j.aca.2016.12.045.

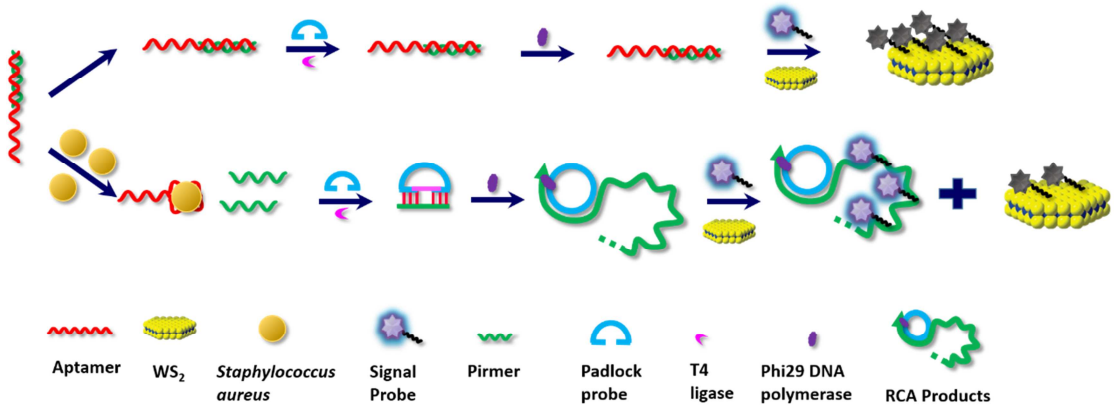

An enhanced chemiluminescence resonance energy transfer aptasensor based on rolling circle amplification and WS_2 nanosheet for *Staphylococcus aureus* detection

Liling Hao[a], Huajie Gu[a], Nuo Duan[a], Shijia Wu[a], Xiaoyuan Ma[a], Yu Xia[a], Zui Tao[a], Zhouping Wang[a,b*]

[a]*State Key Laboratory of Food Science and Technology, School of Food Science and Technology, Jiangnan University, Wuxi 214122, China*

[b]*School of Food Science and Technology, Dalian Polytechnic University, National Engineering Research Center of Seafood, Dalian 116034, China*

* Corresponding author:
Tel & Fax: 86-510-85917023
E-mail: wangzp@jiangnan.edu.cn

Abstract

A chemiluminescence resonance energy transfer aptasensor was fabricated for the detection of *Staphylococcus aureus* (*S. aureus*) with Co^{2+} enhanced N-(aminobutyl)-N-(ethylisoluminol) (ABEI) functional flowerlike gold nanoparticles (Co^{2+}/ABEI-AuNFs) as donor and WS_2 nanosheet as acceptor. In the presence of *S. aureus*, rolling circle amplification (RCA) can be started. Partially complementary sequence of RCA product functional ABEI-AuNFs (cDNA-ABEI-AuNFs) were then annealed to multiple sites of the RCA product to form duplex complex. This complex is less adsorbed onto the WS_2 nanosheet, thus attenuating the quenching of ABEI-AuNFs chemiluminescence by WS_2 nanosheet. In the absence of target *S. aureus* (and hence the absence of RCA and duplex formation), the free cDNA-ABEI-AuNFs is completely adsorbed onto the WS_2 nanosheet and chemiluminescence quenching ensues. Under optimal conditions, the logarithmic correlation between the concentration of *S. aureus* and the CL signal was found to be linear within the range of 50 cfu/mL to 1.5×10^5 cfu/mL ($R^2 = 0.9913$). The limits of detection of the developed method were found to be 15 cfu/mL for *S. aureus*. The selectivity and the capability of the biosensor in meat samples were also studied. Therefore, this simple and easy operation method can be used to detect *S. aureus* with high sensitivity and specificity.

Keywords Rolling Circle Amplification； Co^{2+} enhanced ABEI functional flowerlike gold nanoparticles; WS_2 nanosheet； Chemiluminescence Resonance Energy Transfer； *Staphylococcus aureus*

1. Introduction

Staphylococcus aureus (*S. aureus*) is gram-positive bacterium with a wide distribution. As one of the most common food borne pathogens for humans and animals, *S. aureus* can be able to produce heat-resistant toxins in food[1]. And even trace concentrations of bacteria in food can cause septicemia, osteomyelitis, pneumonia, toxic shock syndrome, and endocarditis [2, 3]. Especially when the infection occurs among certain high risk people such as infants, elderly and chronically ill individuals, the symptoms are more serious [4, 5]. Thus it is critical to develop rapid, sensitive

and selective methods to detect *S. aureus* in food.

There are many kinds of methods to detect *S. aureus*, such as bacteria isolation-culture based conventional methods[6], polymerase chain reaction (PCR) based assays[7, 8] and biosensor based detection methods [9, 10] and so on. According to the detection signal, there are colorimetric[11, 12], fluorescence[13, 14], chemiluminescence(CL)[15, 16], Raman scattering and surface plasmon resonance (SPR) biosensor[17, 18]. Among these optical biosensors, CL biosensors is one kind of promising methods in food safety detection, because in CL reaction, the energy is produced by chemical reactions, and excitation is not needed for sample radiation. So the interference of light scattering, source instability and high backgrounds can be avoided[19].

Among the established CL-based detection methods, CL resonance energy transfer (CRET) is a promising optical detection mode that mainly benefits from the separation-free detection mode and robustness against matrix interferences. CRET involves non-radiative dipole-dipole transfer of energy from a chemiluminescent donor to a suitable acceptor molecule.[20] And the introduction of quantum dots (QDs), grapheme, amorphous carbon nanoparticles[21, 22] and two-dimensional transition metal dichalcogenide (2D-TMDC) nanosheets[23-25] as energy acceptors have made significant progress in the CRET system. Recently, extensive attention has been focused on the 2D-TMDC (e.g., WS_2, etc.) due to their 2D layer structure analogous to graphene. Being an ultrathin direct bandgap semiconductor, WS_2 nanosheet has found widespread applications in catalysis, lithium ion batteries and electrochemical biosensing[26-28].

According to the reports, WS_2 has been applied in fluorescence resonance energy transfer (FRET) assays [29], but the application in CRET was not very common. Jingjin Zhao and Shulin Zhao[25] reported a CRET assay to detect MicroRNA with luminol as the donor and WS_2 nanosheet as acceptor. However, only MicroRNAs or DNA sequences can be detected in that CRET mode. Therefore, in this work, to expand the detection scope, CL reagents functionalized gold nanoparticles (AuNPs) and aptamer were first used in WS_2 nanosheet based CRET assay. Thus, other targets such as antibiotics, food borne pathogens and so on can be detected by the universal CRET assay. Compared with luminol, CL reagents functionalized AuNPs is one of the most

attractive improvements because it can construct the nanosized platform in CL reactions. The nanosized CL platform can combine CL properties of the CL reagents with the unique optical properties, excellent catalytic activity, easy modification as well as good biocompatibility and stability of nanoparticles [30, 31]. And their application can also improve the analytical sensitivity, simplicity, speed, and cost of bioassays. To further improve the sensitivity of the methods, the CL enhancer Co^{2+} and the signal amplification technique rolling circle amplification (RCA) were introduced to the CL system.

There has been some reports that metal irons and CL reagents were co-modified on the surface of gold nanoparticles to enhance the CL intensity [32-34]. However, the reported methods were either tedious and time-consuming for the synthesis or hard for immobilizing recognized molecules such as aptamer on the surface. Therefore, a simpler, easier and more universal method was needed. In our previous study [35], N-(aminobutyl)-N-(ethylisoluminol) (ABEI) and chitosan were used to prepare ABEI functionalized flowerlike gold nanostructures (ABEI-AuNFs) and both of them coexisted on the surface of the nanoparticles. Also, chemically active functional groups of chitosan can strongly interact with divalent metal ions (for example Co^{2+} and Cu^{2+}) through primary amine groups.[36] Thus, CL enhanced Co^{2+}/ABEI-AuNFs can be prepared through the interaction of Co^{2+} and chitosan. In addition, RCA is a simple and efficient molecular amplification technique especially when it combines with aptamer. During the process, long ssDNA with tens to hundreds of tandem repeats can be produced.[37-40] And signal molecules such as fluorescent dye, quantum dots and ABEI-AuNFs and so on can assembled onto the repetitive sequences so that the detection signal can be amplified.

Herein, we report an improved RCA based CRET aptasensor for detecting *S. aureus* by the CRET process between the chemiluminescent donor Co^{2+}/ABEI-AuNFs and chemiluminescent acceptor WS_2 nanosheet. By virtue of CL functional nanoparticles as well as the specific recognition of aptamer, the improved CRET assay are more universal in food safety detection. Co^{2+}/ABEI-AuNFs was first used as CRET donor and first applied in 2D-TMDC based CRET system. In addition, RCA technique was also applied to improve the CL signal in the CRET system for the first time.

2. Materials and methods

2.1 Materials and instruments

A 0.1 M stock solution of ABEI was prepared by dissolving ABEI (TCI (Shanghai) Development Co., Ltd, Shanghai, China) in 0.1 M NaOH solution without further purification and stored at 4□. A $HAuCl_4$ stock solution (0.2% $HAuCl_4$, w/v) was prepared by dissolving $HAuCl_4 \cdot 4H_2O$ (Shanghai Reagent, Shanghai, China) in purified water and stored at 4□. P-Iodophenol (PIP) (purity >98.0%) and tris (2-carboxyethyl) phosphine hydrochloride (TCEP) (purity >98.0%) were purchased from TCI (Shanghai) Development Co., Ltd (Shanghai, China). Chitosan was purchased from Sigma-Aldrich Shanghai Trading Co., Ltd, (Shanghai, China). The tungsten disulfide (WS_2) nanosheet was purchased from Nanjing XFNano Material Tech Co., Ltd. (Nanjing, China). H_2O_2 used in detecting buffer were freshly prepared daily from 30% (v/v) H_2O_2 (Xinke Electrochemical Reagent Factory, Bengbu, China). All other reagents used in this study were of analytical grade. The oligonucleotides used in this work (synthesized by Shanghai Sangon Biological Science & Technology Company, Shanghai, China) were shown in Table 1. The meat tested in this work was bought form local market. Ultrapure water was prepared with a Millipore Milli-Q system and was used throughout the study.

Table 1 DNA sequences used in the work

Oligonucleotides	Sequences
Aptamer	5′-GCAATGGTACGGTACTTCCTCGGCACGTTCTCAGTAGCGCTCGCTGGTC ATCCCACAGCTACGTCAAAAGTGCACGCTACTTTGCTAA-3′
Primer	5′-TTAGCAAAGTAGCGTGCACTT-3′
Padlock template	5′-PO_4-TACTTTGCTAATATATGATGGTACCGCAGTATGAGTATCTCCTATCAC TACTAAGTGGAAGAAATGAAGTGCACGC-3′
Detection probe	5′-TGCACGCTACTTTGCTTTTTT-$(CH_2)_6$-SH-3′

Transmission electron microscopy (TEM) and energy dispersive spectra (EDS) were performed using a JEOL model 2100HR instrument operating at 200 kV accelerating voltage (TEM, JEOL Ltd., Japan). Ultraviolet-visible (UV-vis) absorption spectra were recorded using a UV-1800 spectrophotometer (Shimadzu, Japan). The surface analysis of WS_2 nanosheet was characterized

by a Dimension Icon Atomic Force Microscope System (AFM, Bruker Co., Germany). The electrophoresis experiment was carried out with Western Electrophoresis apparatus (BIO-RAD, USA). The CL measurement was conducted on a static injection CL system consisting of a model MPI-M CL detector and a model multifunctional CL detector (Xi'an Remex Analytical Instrument Co., Ltd.). The graphics program used in this work was Origin Pro 2015.

2.2 Bacterial strains and culture media

Staphylococcus aureus (*S. aureus*) ATCC 29213, *Salmonella typhimurium* (*S. typhimurium*) ATCC 14028, *Escherichia coli* (*E. coli*) ATCC 25922 were obtained from the American Type Culture Collection (ATCC). *Listeria monocytogenes* (*L. monocytogenes*), *Bacillus cereus* (*B. cereus*) were kindly provided by the Animal, Plant and Food Inspection Centre, Jiangsu Entry-Exit Inspection and Quarantine Bureau (Nanjing, China). The bacteria were grown in Luria-Bertani (LB) (BD Difco) until an OD600 of 0.3 was obtained. The bacteria cells were pelleted at 4000 rpm and 4°C and then washed twice in 0.01 M phosphate buffer solution (PB) (pH 7.4) at room temperature.

2.3 Synthesis of ABEI-AuNFs and Co^{2+} enhanced donor

ABEI-AuNFs were synthesized by reducing $HAuCl_4$ with ABEI and chitosan according to the method of Wang and Cui [41] with some modifications. ABEI-AuNFs were typically synthesized by first dissolving 0.075 g of chitosan in 25 mL of acetic acid solution (HAc, 2% v/v). Then, 3.0 mL of the ABEI stock solution was added, afterwards, the mixture was diluted to 43 mL and heated to boil under vigorous stirring. Next, 8 mL of $HAuCl_4$ stock solution was added dropwise, and the mixture was maintained at the boiling point under vigorous stirring for 1 h. The flask was then allowed to cool naturally to room temperature, and the mixture was stored at 4°C for further use.

Before the subsequent characterization and modification, the centrifugation–ultrasonic dispersion process was used to remove the inorganic or organic impurities. And then the prepared gold nanoparticles were characterized by TEM. The thiolated hybridized complementary strand

modified ABEI-AuNFs signal probes were fabricated according to the method of Li and Cui [42] with some modifications. First, 5 mL of the as-prepared mixture was centrifuged at 10,000 rpm for 10 min, and the precipitates were suspended with 1.5 mL of 30 mM Tris–HCl (pH 7.4) to obtain an ABEI-AuNFs colloid. Subsequently, 45 µL of 10 µM thiolated aptamer complementary strand and 45 µL of 10 µM TCEP were added to the ABEI-AuNFs colloid and incubated at room temperature for 24 h. Then, 100 µL 30 mM Co^{2+} solution was added to the mixture kept for 30 min at room temperature. Finally, the resulting solution was centrifuged at a speed of 10000 rpm for 10 min. After the supernatant was removed, the soft precipitant was dispersed in 1.5 mL PB for further use. And EDS analysis was then performed to verify the formation of Co^{2+} enhanced signal probes.

2.4 RCA reaction procedures

50 µL of 10^{-6} M aptamer and 50 µL of 10^{-6} M primer was mixed and degenerated at 95°C for 10 min then hybridized with gradient cooling to obtain hybridized product, and the ramp rate was set as 0.1°C s^{-1}. Afterwards, 100 µL of the *S. aureus* and 10 µL of the prepared hybridized product were mixed and incubated at 37°C for 30 min. Subsequently, 10 µL of 10^{-6} M padlock probe and 1.25 µL T4 DNA ligase (5.0 U μL^{-1}) were added and incubated at 37°C for 60 min. And 2.5 µL 5 mM dNTPs and 2.5 µL 10 U μL^{-1} Phi29 DNA polymerase were added and incubated at 37°C for 90 min. After RCA reaction, the solution was immerged in the thermostatic water bath at 75°C for 15 minutes to devitalize the enzymes.

Gel electrophoresis was used to characterize the RCA product. The electrophoresis experiment was performed by 0.7% agarose gels and run in 1× TAE buffer (0.04 mol L^{-1} Tris, 0.02 mol L^{-1} HAc, 0.01 mol L^{-1} EDTA, pH 8.0) at room temperature under a constant voltage of 100 V for 60 min with loading of 5 µL of each sample into the lanes.

2.5 Analytical procedure

S. aureus were determined as follows. First, the concentrations of the *S. aureus* was determined by

plate counting methods, 100 μL of the sample solution containing different concentrations of the *S. aureus* and 10 μL of the prepared hybridized product were mixed to start RCA reaction. After that, 500 μL of Co^{2+} enhanced signal probes were added to 10 μL of the RCA product and incubated for 30 min. Finally, 0.5 mL of 0.2 mg mL^{-1} WS_2 nanosheet was added and the CL intensity was measured after 20 min. In CL detection, 100 μL the above solution and 200 μL of the detecting buffer (0.2 mol L^{-1} H_2O_2, 0.05 mol L^{-1} PIP, 0.00095 mol L^{-1} Na_2HPO_4•$2H_2O$, 0.00405 mol L^{-1} NaH_2PO_4•$12H_2O$ and 0.1 mol L^{-1} NaOH) were added into the wells and the CL intensity was determined after 500 s. All the measurements were done in triplicate.

2.6 Sample preparation

5 g pork paste was added into 10 mL PB and sterilized. And the mixture was centrifuged at 10000 rpm for 15 min, the solid impurities was removed. Then gradient dilutions of *S. aureus* were added to the supernatant. The prepared sample was used for relative standard deviation (RSD) detection and standard addition and recovery experiments.

2. Results and discussion

3.1 Principle of the CRET aptasensor

Preferred position for Scheme.1

The CRET aptasensor for the detection of *S. aureus* based on the Co^{2+}/ABEI-AuNFs and WS_2 nanosheet is illustrated in Scheme 1. The aptamer of *S. aureus* and primer of RCA is partially complemented, and in the presence of *S. aureus*, the aptamer tends to combine with the target thus leading to the melting of DNA duplex. When adding padlock probe that is complementary to the primer, RCA reaction could be initiated in the presence of T4 DNA ligase, Phi29 DNA polymerase and dNTPs, producing hundreds of tandem-repeat sequences. Signal probes (Co^{2+}/ABEI-AuNFs-cDNA) are then annealed to multiple sites of the RCA product (RCAP) to form Co^{2+}/ABEI-AuNFs-cDNA-/RCAP duplex complex. And the duplex molecule cannot be adsorbed onto the WS_2 nanosheet surface because of its weak affinity. In this case, the signal

probes are less adsorbed onto the WS_2 nanosheet, thus attenuating the quenching of ABEI-AuNFs chemiluminescence by WS_2 nanosheet. In the absence of target *S. aureus* (and hence the absence of RCA and duplex formation), the free signal probes can be completely adsorbed onto the WS_2 nanosheet and chemiluminescence quenching ensues. Thus after CRET between the donor (Co^{2+}/ABEI-AuNFs) and acceptor (WS_2 nanosheet), highly specific and sensitive detection of *S. aureus* was achieved by measuring the CL signal of the reaction system. And the CL intensity was positive correlation with the concentration of *S. aureus*.

3.2 Characteristics of the donor

In the coexistence of certain concentration of ABEI and chitosan, $HAuCl_4$ can be reduced to form flowerlilke nanoparticles with larger specific surface area than that of spherical gold nanoparticles thus resulting higher CL intensity. The exact morphology of ABEI-AuNFs was measured by TEM. Fig. 1 shows a TEM image of ABEI-AuNFs with a typical flowerlilke shape.

Preferred position for Fig. 1

The thiolated complementary strand (cDNA) of RCAP and ABEI-AuNFs were linked through the Au-S covalent bond with TCEP as a reducer. UV-vis absorption spectroscopy was used to verify the conjugation. As shown in Fig. S1, the decrease in UV-vis absorption spectrum at about 260 nm before (a) and after (b) incubation of oligonucleotides and ABEI-AuNFs indicates that some oligonucleotides has been linked on the surface of ABEI-AuNFs.

Energy dispersive spectroscopy (EDS) was used to characterize the formation of Co^{2+}/ABEI-AuNFs-cDNA. According to the EDS analysis (Fig. 2), the intense peaks corresponding to the Co and Au elements could be directly used to identify the existence of Co^{2+} on the surface of AuNFs. As a common CL enhancer, Co^{2+} has been used to catalyze the CL reactions of luminol and its analogues with H_2O_2[43]. The catalysis of Co^{2+} in the steady-state CL system was also investigated. Fig. S2 shows that the CL intensity of Co^{2+} enhanced system (a) was about 30 times higher than that of without Co^{2+} (b).

Preferred position for Fig. 2

3.3 Characteristics of WS_2 nanosheet and RCA product

TEM and AFM were used to characterize the WS_2 nanosheet (Fig. S3). The AFM characterization shows that the thickness of a WS_2 nanosheet is about 1 nm, indicating that the WS_2 nanosheet used here is monolayer[44].

Furthermore, the UV-vis absorption spectroscopy of WS_2 nanosheet was measured. And results showed that WS_2 nanosheet exhibits broad absorption which is largely overlapped with the CL spectrum generated from ABEI-AuNFs-H_2O_2 CL system (Fig. S4). The result implies that ABEI-AuNFs and the WS_2 nanosheet can act as a nice pair of CRET donors/acceptors.

The RCA reaction consists of two processes. In the first step, the aptamer and primer were hybridized, and then the adding of *S. aureus* can cause the melting of DNA duplex to produce free primer. In the second step, the padlock probe and T4 ligase were added, the free primer and padlock probe can hybridize and then form a closed circular DNA with the assistance of T4 ligase. Afterwards, a linear RCA reaction can be initiated in the presence of Phi29 DNA polymerase and dNTPs, producing hundreds of tandem-repeat sequences.

The agarose gel electrophoresis experiment was performed to verify the RCA reaction. The results are shown in Fig. 3, a bright band was observed in the presence of *S. aureus*. According to the indication of the marker (250-15000 bp) (lane 1), the number of the bases contained in the RCA product (lane 2 and 3) was estimated to be much higher than 15 000 bp, indicating that the RCA reaction successfully occurred. Compared with lane 2 and 3, lane 4 and 5 displayed no bands in the absence of *S. aureus*, indicating that the RCA reaction was not triggered.

Preferred position for Fig. 3

3.4 Optimization for the assay

The effect of concentration of WS_2 nanosheet on CL intensity was also studied (Fig. S5). With the increasing concentration of WS_2, the quenching efficiency was enhanced and the CL intensity decreased gradually. This is ascribed to the spectral overlapping of CL and the absorption characteristics of WS_2. Results showed that the largest CL quenching was obtained when the WS_2 nanosheet concentration was 0.2 mg mL^{-1}. And the incubation time of Co^{2+}/ABEI-AuNFs-cDNA-/RCAP duplex molecules and WS_2 nanosheet was optimized (Fig. S6).The optimal incubation time was 20 min that may because the CRET need some time to reach dynamic equilibrium.

Additionally, during the assay, the content of RCA product that react with Co^{2+}/ABEI-AuNFs-cDNA also played key roles. The effect of RCA product content on CL intensity was studied in the range of 5 to 15 μL with *S. aureus* concentration of 1.5×10^4 cfu mL^{-1}(Fig. S7). This may because the optimal combination of Co^{2+}/ABEI-AuNFs-cDNA and RCA product can be reached when the added of RCA product was 10 μL.

3.5 Analytical performance

With the increase of gradient concentrations of *S. aureus* in the detection system, the RCA product concentration increased and the CL quenching decreased thus the gradual increase of CL signals was observed (Fig. 4). Under the above optimal conditions, the ΔCL intensity ($\Delta CL=CL-CL_0$, CL and CL_0 represent the CL intensity in the presence of *S. aureus* and the minimum background CL intensity respectively) was linear positive correlation with logarithm of the concentration of *S. aureus*. The linear range of the relationship varied from 50 cfu mL^{-1} to 1.5×10^5 cfu mL^{-1} (Y = -507.20+368.24*X, R = 0.9913). Statistical analysis revealed that the detection limit of *S. aureus* is equal to 15 cfu mL^{-1}, as estimated by using 3σ. Some different detection methods for S. aureus are also presented in Table 2, the limit of detection of the developed bioassay is lower than most of these methods. The precision expressed as the relative standard deviation (RSD) of *S. aureus* detection was equal to 3.72% (1.5×10^4 cfu mL^{-1}, n = 7) indicating that the developed method exhibited good reproducibility.

Preferred position for Fig. 4

Table 2. The current detection methods for *S. aureus*

Methods	Nanomaterial/recognized molecule	LOD	References
Colorimetric assay	AuNPs/protein	19 cfu mL^{-1}	[12]
Surface-enhanced Raman spectroscopy assay	Fe_3O_4 magnetic gold nanoparticles/aptamer	35 cfu mL^{-1}	[18]
Electrode piezoelectric quartz crystal assay	Graphene/aptamer	41 cfu mL^{-1}	[45]
Fluorescence assay	Upconversion nanoparticles/aptamer	25 cfu mL^{-1}	[46]
Electrochemical assay	AgNPs/aptamer	1.0 cfu mL^{-1}	[47]
Electrochemiluminescent assay	Graphene/antibody	310 cfu mL^{-1}	[48]

3.6 Specificity Evaluation

To assess the specificity of the developed CRET aptasenor for *S. aureus*, the influences of some other pathogenic bacteria including *E. coli* (a), *S. typhimurium* (b), *B. cereus* (c) and *L. monocytogenes* (d) were selected and tested under the same experimental conditions as those for *S. aureus* (e). ΔCL ratio was used to evaluate the specificity of the aptasonsor where ΔCL ratio equals $(CL-CL_0)/CL_A$ and CL_A represents the CL intensity of *S. aureus*, CL_0 represents the CL intensity of blank sample. Therefore, the smaller the ΔCL ratio is, the less the CL change caused by nonspecific binding. As illustrated in Fig. 5, the response induced by the non-specific binding was negligible compared to the response induced by the target bacteria. These results demonstrate that the developed method has excellent selectivity for *S. aureus* due to the high affinity and specificity advantage of the aptamer.

Preferred position for Fig. 5

3.7 Analytical Application in pork samples

Feasibility and reliability of the proposed biosensor for practical applications was further confirmed by determining *S. aureus* in pork samples by spiking the samples with specific amounts of *S. aureus*. The sample was tested using the proposed method and the classical plate counting

methods. The results are summarized in Table 3; there was no significant difference between the results obtained via the proposed method and those obtained through the standard plate method. The recoveries of CL measurements of spiked real samples ranged from 94.7 to 102.0%, indicating good accuracy of the developed aptamer-based CL detection for *S. aureus*.

Table. 3 Comparison of the pork sample results obtained from the developed method and classical plate counting method

Sample	Added concentration (cfu mL^{-1})	Plate counting of *S. aureus* (cfu mL^{-1})	Measured concentration (cfu mL^{-1})	Recovery ratio obtained by the developed method (%)
Pork	1.5×10^{2}	$(1.45\pm0.17)\times10^{2}$	$(1.42\pm0.15)\times10^{2}$	94.7%
Pork	1.5×10^{3}	$(1.56\pm0.16)\times10^{3}$	$(1.53\pm0.13)\times10^{3}$	102.0%
Pork	1.5×10^{4}	$(1.43\pm0.21)\times10^{4}$	$(1.46\pm0.18)\times10^{4}$	97.3%

4. Conclusion

In this work, a novel steady-state CRET aptasensor using Co^{2+}/ABEI-AuNFs as donor and WS_2 nanosheet as acceptor was introduced for detection of *S. aureus* with high sensitivity, selectivity and easy operation. In the absence of *S. aureus*, the RCA reaction cannot be triggered, and the CL of signal probes can be quenched by WS_2 nanosheet. While the presence of *S. aureus* can cause the melting of the aptamer-primer DNA duplex, and then RCA can be started. Signal probes was then assembled on the RCAP to form a Co^{2+}/ABEI-AuNFs-cDNA-/RCAP duplex complex, thus attenuating the quenching of ABEI-AuNFs chemiluminescence by WS_2 nanosheet. And the CL intensity was positive correlation with the concentration of *S. aureus*. During the process, the introduction of ABEI-AuNFs and aptamer to the improved WS_2 nanosheet based CRET system can significantly expand the field of detection application to make it more than just detection of MicroRNAs or DNA sequences. The improved CRET system can realize the detection of other foodborne pathogenic bacteria and even undesirable small molecule just by the replacement with other aptamer. Furthermore, the introduction of CL enhancer Co^{2+} and the signal amplification RCA technique can also improve the sensitivity of the biosensor.

Acknowledgments

This work was partly supported by the National S&T Support Program of China (2015BAD17B02), NSFC (21375049), Key Research and Development Program of Jiangsu Province (BE2016306), BK20140155, National Natural Science Foundation of China (31401576) and Synergetic Innovation Center of Food Safety and quality control of Jiangsu Province.

References

[1] H.F.L. Wertheim, D.C. Melles, M.C. Vos, W. van Leeuwen, A. van Belkum, H.A. Verbrugh, J.L. Nouwen, The role of nasal carriage in Staphylococcus aureus infections, The Lancet Infectious Diseases, 5 (2005) 751-762.

[2] R.J. Gorwitz, D. Kruszon-Moran, S.K. McAllister, G. McQuillan, L.K. McDougal, G.E. Fosheim, B.J. Jensen, G. Killgore, F.C. Tenover, M.J. Kuehnert, Changes in the Prevalence of Nasal Colonization with Staphylococcus aureus in the United States, 2001–2004, Journal of Infectious Diseases, 197 (2008) 1226-1234.

[3] F.D. Lowy Staphylococcus aureus Infections, New England Journal of Medicine, 339 (1998) 520-532.

[4] A.A. Wieneke, D. Roberts, R.J. Gilbert, Staphylococcal food poisoning in the United Kingdom, 1969–90, Epidemiology and Infection, 110 (2009) 519-531.

[5] J.L. Smith, Foodborne illness in the elderly, J. Food Prot. , 61 (1998) 1229-1239.

[6] F. Ampe, N. Ben Omar, C. Moizan, C. Wacher, J.P. Guyot, Polyphasic study of the spatial distribution of microorganisms in Mexican pozol, a fermented maize dough, demonstrates the need for cultivation-independent methods to investigate traditional fermentations, Applied and Environmental Microbiology, 65 (1999) 5464-5473.

[7] D.K. Warren, R.S. Liao, L.R. Merz, M. Eveland, W.M. Dunne, Detection of methicillin-resistant Staphylococcus aureus directly from nasal swab specimens by a real-time PCR assay, J. Clin. Microbiol. , 42 (2004) 5578-5581.

[8] F. Forghani, S. Wei, D.H. Oh, A Rapid Multiplex Real-Time PCR High-Resolution Melt Curve Assay for the Simultaneous Detection of Bacillus cereus, Listeria monocytogenes, and Staphylococcus aureus in Food, J. Food Prot. , 79 (2016) 810-815.

[9] Y. Sun, X. He, J. Ji, M. Jia, Z. Wang, X. Sun, A highly selective and sensitive electrochemical CS–MWCNTs/Au-NPs composite DNA biosensor for Staphylococcus aureus gene sequence detection, Talanta, 141 (2015) 300-306.

[10] A. Purwidyantri, C.-H. Chen, B.-J. Hwang, J.-D. Luo, C.-C. Chiou, Y.-C. Tian, C.-Y. Lin, C.-H. Cheng, C.-S. Lai, Spin-coated Au-nanohole arrays engineered by nanosphere lithography for a Staphylococcus aureus 16S rRNA electrochemical sensor, Biosens. Bioelectron. , 77 (2016) 1086-1094.

[11] M.S. Verma, J.L. Rogowski, L. Jones, F.X. Gu, Colorimetric biosensing of pathogens using gold nanoparticles, Biotechnol. Adv. , 33 (2015) 666-680.

[12] P. Liu, L. Han, F. Wang, V.A. Petrenko, A. Liu, Gold nanoprobe functionalized with specific fusion protein selection from phage display and its application in rapid, selective and sensitive colorimetric biosensing of Staphylococcus aureus, Biosens. Bioelectron. , 82 (2016) 195-203.

[13] J. Shi, C. Chan, Y. Pang, W. Ye, F. Tian, J. Lyu, Y. Zhang, M. Yang, A fluorescence resonance energy transfer (FRET) biosensor based on graphene quantum dots (GQDs) and gold nanoparticles (AuNPs) for the detection of mecA gene sequence of Staphylococcus aureus, Biosens. Bioelectron. , 67 (2015)

595-600.

[14] W. Kong, J. Xiong, H. Yue, Z. Fu, Sandwich fluorimetric method for specific detection of Staphylococcus aureus based on antibiotic-affinity strategy, Anal. Chem. , 87 (2015) 9864-9868.

[15] J. Xiong, W. Wang, Y. Zhou, W. Kong, Z. Wang, Z. Fu, Ultra-sensitive chemiluminescent detection of Staphylococcus aureus based on competitive binding of Staphylococcus protein A-modified magnetic beads to immunoglobulin G, Microchim. Acta 183 (2016) 1507-1512.

[16] H. Gao, S. Yang, J. Han, J. Xiong, W. Kong, C. Li, G. Liao, Z. Fu, Double-site recognition of pathogenic bacterial whole cells based on an antibiotic-affinity strategy, Chem Commun (Camb), 51 (2015) 12497-12500.

[17] N. Tawil, F. Mouawad, S. Lévesque, E. Sacher, R. Mandeville, M. Meunier, The differential detection of methicillin-resistant, methicillin-susceptible and borderline oxacillin-resistant Staphylococcus aureus by surface plasmon resonance, Biosens. Bioelectron. , 49 (2013) 334-340.

[18] H. Zhang, X. Ma, Y. Liu, N. Duan, S. Wu, Z. Wang, B. Xu, Gold nanoparticles enhanced SERS aptasensor for the simultaneous detection of Salmonella typhimurium and Staphylococcus aureus, Biosens. Bioelectron. , 74 (2015) 872-877.

[19] C. Dodeigne, L. Thunus, R. Lejeune, Chemiluminescence as diagnostic tool. A review, Talanta, 51 (2000) 415-439.

[20] X.Y. Huang, L. Li, H.F. Qian, C.Q. Dong, J.C. Ren, A resonance energy transfer between chemiluminescent donors and luminescent quantum-dots as acceptors (CRET), Angewandte Chemie-International Edition, 45 (2006) 5140-5143.

[21] Z. Wang, H. Gao, Z. Fu, Introducing novel amorphous carbon nanoparticles as energy acceptors into a chemiluminescence resonance energy transfer immunoassay system, Analyst, 138 (2013) 6753-6758.

[22] H. Gao, W. Wang, Z. Wang, J. Han, Z. Fu, Amorphous carbon nanoparticle used as novel resonance energy transfer acceptor for chemiluminescent immunoassay of transferrin, Anal. Chim. Acta 819 (2014) 102-107.

[23] R. Freeman, X. Liu, I. Willner, Chemiluminescent and Chemiluminescence Resonance Energy Transfer (CRET) Detection of DNA, Metal Ions, and Aptamer–Substrate Complexes Using Hemin/G-Quadruplexes and CdSe/ZnS Quantum Dots, J. Am. Chem. Soc. , 133 (2011) 11597-11604.

[24] J.S. Lee, H.-A. Joung, M.-G. Kim, C.B. Park, Graphene-Based Chemiluminescence Resonance Energy Transfer for Homogeneous Immunoassay, ACS Nano, 6 (2012) 2978-2983.

[25] J. Zhao, X. Jin, M. Vdovenko, L. Zhang, I.Y. Sakharov, S. Zhao, A WS2 nanosheet based chemiluminescence resonance energy transfer platform for sensing biomolecules, Chem Commun (Camb), 51 (2015) 11092-11095.

[26] J. Yang, D. Voiry, S.J. Ahn, D. Kang, A.Y. Kim, M. Chhowalla, H.S. Shin, Two-Dimensional Hybrid Nanosheets of Tungsten Disulfide and Reduced Graphene Oxide as Catalysts for Enhanced Hydrogen Evolution, Angewandte Chemie-International Edition, 52 (2013) 13751-13754.

[27] R. Bhandavat, L. David, G. Singh, Synthesis of Surface-Functionalized WS2 Nanosheets and Performance as Li-Ion Battery Anodes, J. Phys. Chem. Lett. , 3 (2012) 1523-1530.

[28] K.J. Huang, L. Wang, Y.J. Liu, T. Gan, Y.M. Liu, L.L. Wang, Y. Fan, Synthesis and electrochemical performances of layered tungsten sulfide-graphene nanocomposite as a sensing platform for catechol, resorcinol and hydroquinone, Electrochim. Acta 107 (2013) 379-387.

[29] Q. Xi, D.M. Zhou, Y.Y. Kan, J. Ge, Z.K. Wu, R.Q. Yu, J.H. Jiang, Highly sensitive and selective strategy for microRNA detection based on WS2 nanosheet mediated fluorescence quenching and

duplex-specific nuclease signal amplification, Anal. Chem. , 86 (2014) 1361-1365.
[30] S. Bi, H. Zhou, S. Zhang, A novel synergistic enhanced chemiluminescence achieved by a multiplex nanoprobe for biological applications combined with dual-amplification of magnetic nanoparticles, Chemical Science, 1 (2010) 681.
[31] T. Peterle, P. Ringler, M. Mayor, Gold Nanoparticles Stabilized by Acetylene-Functionalized Multidentate Thioether Ligands: Building Blocks for Nanoparticle Superstructures, Adv. Funct. Mater. , 19 (2009) 3497-3506.
[32] J. Shu, W. Wang, H. Cui, Direct electrochemiluminescence of gold nanoparticles bifunctionalized by luminol analogue-metal complexes in neutral and alkaline media, Chem Commun (Camb), 51 (2015) 11366-11369.
[33] F. Li, Y. Liu, M. Zhuang, H. Zhang, X. Liu, H. Cui, Biothiols as chelators for preparation of N-(aminobutyl)-N-(ethylisoluminol)/Cu(2+) complexes bifunctionalized gold nanoparticles and sensitive sensing of pyrophosphate ion, ACS Appl Mater Interfaces, 6 (2014) 18104-18111.
[34] B. Khadro, B.D. Leca-Bouvier, F. Lagarde, F. Barbier, L.J. Blum, C. Martelet, L. Marcotte, M. Tabrizian, N. Jaffrezic-Renault, Chemiluminescence of Luminol for the Determination of Cobalt(II) Adsorbed on a Chitosan Membrane, Sensor Letters, 7 (2009) 833-838.
[35] L. Hao, N. Duan, S. Wu, B. Xu, Z. Wang, Chemiluminescent aptasensor for chloramphenicol based on N-(4-aminobutyl)-N-ethylisoluminol-functionalized flower-like gold nanostructures and magnetic nanoparticles, Anal Bioanal Chem, 407 (2015) 7907-7915.
[36] M.-W. Wan, C.-C. Kan, B.D. Rogel, M.L.P. Dalida, Adsorption of copper (II) and lead (II) ions from aqueous solution on chitosan-coated sand, Carbohydr. Polym. , 80 (2010) 891-899.
[37] W. Zhao, M.M. Ali, M.A. Brook, Y. Li, Rolling circle amplification: applications in nanotechnology and biodetection with functional nucleic acids, Angew Chem Int Ed Engl, 47 (2008) 6330-6337.
[38] M.M. Ali, F. Li, Z. Zhang, K. Zhang, D.K. Kang, J.A. Ankrum, X.C. Le, W. Zhao, Rolling circle amplification: a versatile tool for chemical biology, materials science and medicine, Chem. Soc. Rev. , 43 (2014) 3324-3341.
[39] H. Kuhn, V.V. Demidov, M.D. Frank-Kamenetskii, Rolling-circle amplification under topological constraints, Nucleic Acids Res. , 30 (2002) 574-580.
[40] Q. Guo, X. Yang, K. Wang, W. Tan, W. Li, H. Tang, H. Li, Sensitive fluorescence detection of nucleic acids based on isothermal circular strand-displacement polymerization reaction, Nucleic Acids Res. , 37 (2009) e20.
[41] W. Wang, H. Cui, Chitosan-luminol reduced gold nanoflowers: From one-pot synthesis to morphology-dependent SPR and chemiluminescence sensing, J. Phys. Chem. C 112 (2008) 10759-10766.
[42] F. Li, H. Cui, A label-free electrochemiluminescence aptasensor for thrombin based on novel assembly strategy of oligonucleotide and luminol functionalized gold nanoparticles, Biosensors & Bioelectronics, 39 (2013) 261-267.
[43] M.P. Neary, R. Seitz, D.M. Hercules, A Chemiluminescence Detector for Transition Metals Separated by Ion Exchange, Anal. Lett. , 7 (1974) 583-590.
[44] Y. Yuan, R. Li, Z. Liu, Establishing water-soluble layered WS(2) nanosheet as a platform for biosensing, Anal. Chem. , 86 (2014) 3610-3615.
[45] Y. Lian, F. He, H. Wang, F. Tong, A new aptamer/graphene interdigitated gold electrode piezoelectric sensor for rapid and specific detection of Staphylococcus aureus, Biosens. Bioelectron. , 65 (2015) 314-319.

[46] S. Wu, N. Duan, Z. Shi, C. Fang, Z. Wang, Simultaneous aptasensor for multiplex pathogenic bacteria detection based on multicolor upconversion nanoparticles labels, Anal. Chem. , 86 (2014) 3100-3107.

[47] A. Abbaspour, F. Norouz-Sarvestani, A. Noori, N. Soltani, Aptamer-conjugated silver nanoparticles for electrochemical dual-aptamer-based sandwich detection of staphylococcus aureus, Biosens. Bioelectron. , 68 (2015) 149-155.

[48] H. Yue, Y. Zhou, P. Wang, X. Wang, Z. Wang, L. Wang, Z. Fu, A facile label-free electrochemiluminescent biosensor for specific detection of Staphylococcus aureus utilizing the binding between immunoglobulin G and protein A, Talanta, 153 (2016) 401-406.

Figure captions:

Scheme. 1 Schematic illustration of the CRET biosensor for the detection of *S. aureus* based on Co^{2+}/ABEI-AuNFs and WS_2 nanosheet.

Fig. 1 TEM image of ABEI-AuNFs.

Fig. 2 EDS of Co^{2+} enhanced ABEI-AuNFs.

Fig. 3 Results of agarose gel electrophoresis experiment for the verification of RCA products.

Fig. 4 Standard curve of the CL intensity versus logarithm concentration of *S. aureus* measured by the developed method.

Fig. 5 Specificity investigation of the CL aptasensor for *S. aureus*, a: *E. coli*, b: *S. typhimurium*, c: *B. cereus*, d: *L. monocytogenes* and e: *S. aureus.*

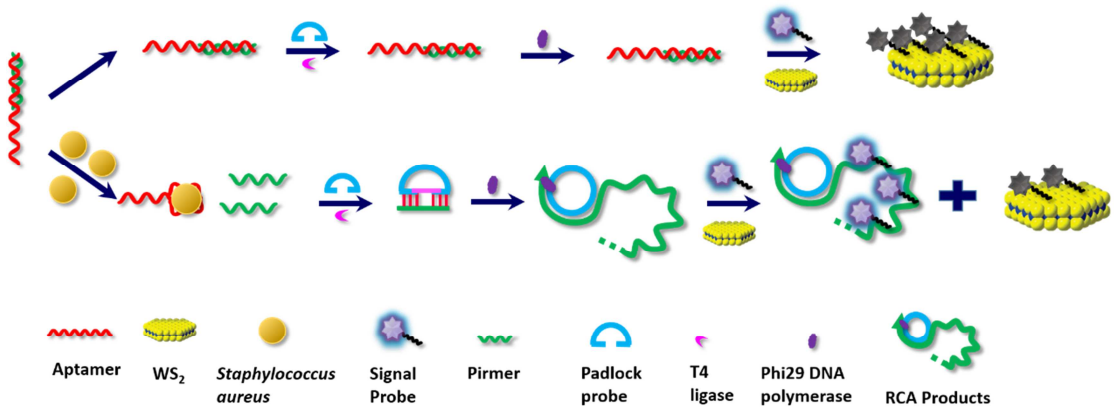

Scheme. 1

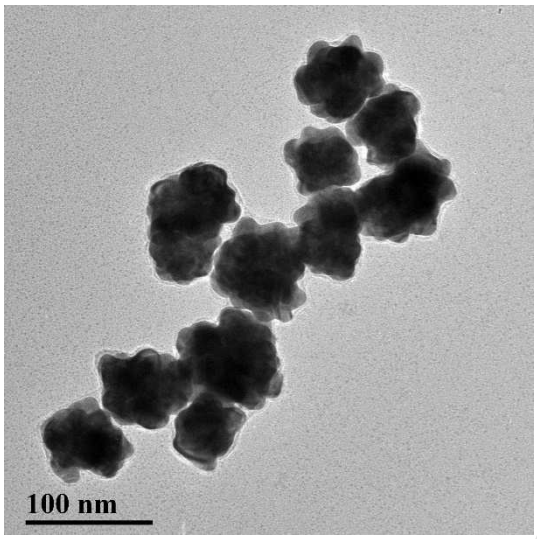

Fig. 1

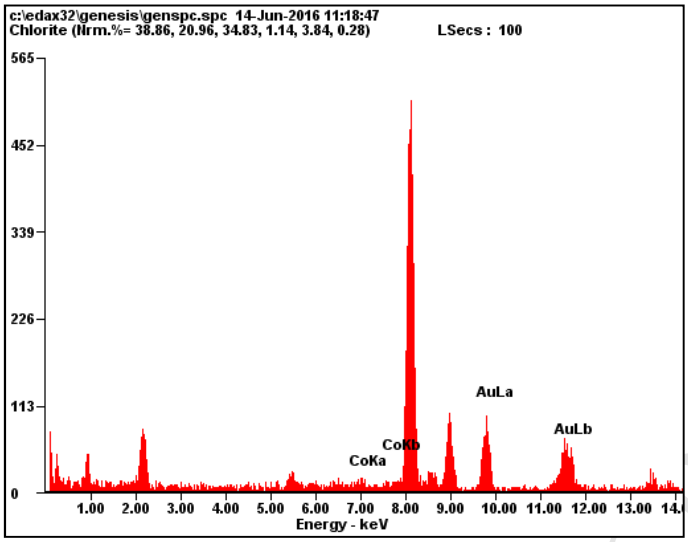

Fig. 2

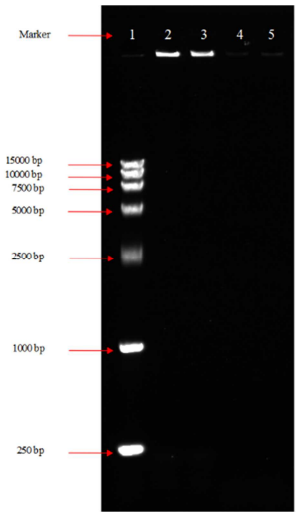

Fig. 3.

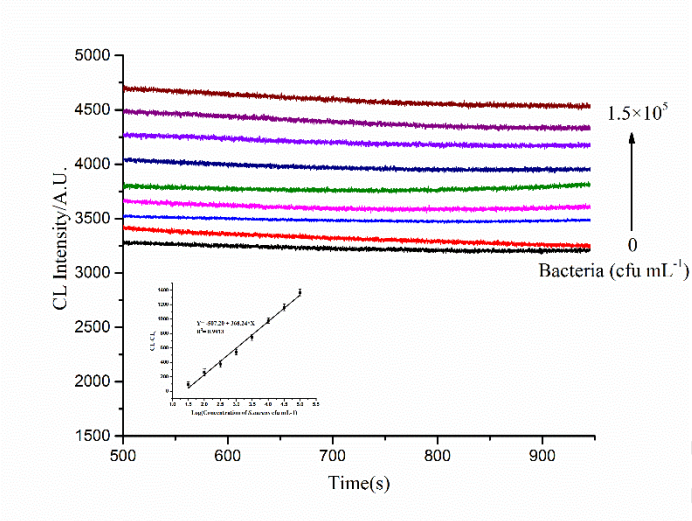

Fig. 4.

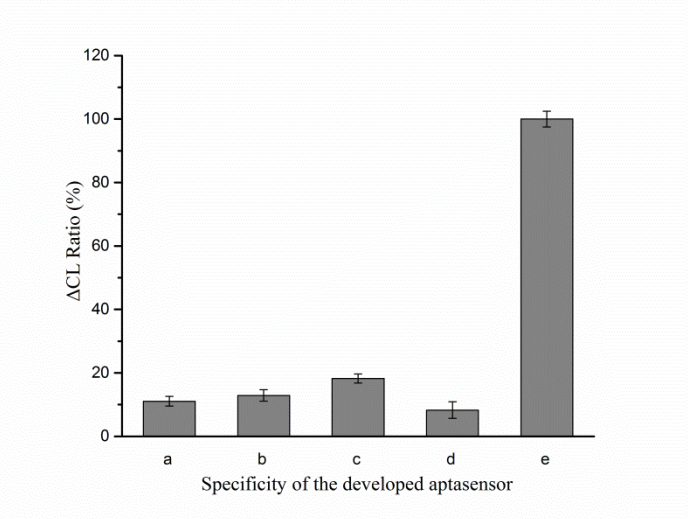

Fig. 5.

Highlights:

- Co^{2+} enhanced ABEI functional flowerlike gold nanoparticles (Co^{2+}/ABEI-AuNFs) was first used as chemiluminescent donor.
- Rolling circle amplification (RCA) technique was also applied in the WS_2 nanosheet based CRET system for the first time.
- The improved WS_2 nanosheet based CRET platform can overcome the limitation that only DNA or RNA can be detected and expand the detection scope.
- A steady-state CRET aptasensor based on P-Iodophenol (PIP) and RCA was fabricated to detect *S. aureus* with high sensitivity and specificity.